International Journal of Bifurcation and Chaos

Modeling and Analysis of the Multi-annual Cholera Outbreaks With Host-pathogen Encounters

Wenjing Zhang*
Department of Mathematics and Statistics
Texas Tech University, Lubbock, Texas, USA
wenjing.zhang@ttu.edu

Received (to be inserted by publisher)

Re-emergence of cholera threatens people's health globally. However, its periodic re-emerging outbreaks are still poorly understood. In this paper, we develop a simple ordinary differential equation (ODE) model to study the cholera outbreak cycles. Our model involves both direct (i.e., human-to-human) and indirect (i.e., environment-to-human) transmission routes, due to the multiple interactions between the human host, the pathogen, and the environment. In particular, we model the pathogen searching distance as a Poisson point process, and then formulate the host-pathogen encounter (HPE) rate. A thorough mathematical analysis is performed to investigate local and global dynamics of the model. Necessary and sufficient condition under which the backward bifurcation occurs is derived. Fold, Hopf, and Bogdanov-Takens bifurcations are studied with original model parameter values to reveal their relations with model behaviors. One- and two-dimensional bifurcation diagrams are provided to categorize model dynamics with respect to its parameter values. Analytical and numerical analyses show that our simple model is sufficient to exhibit complex epidemic patterns of cholera dynamics including bi-stability and annual and multi-annual periodic outbreak. Our result regarding the backward bifurcation and complex dynamics of cholera epidemics highlight the challenges in the prevention and control of the disease.
Keywords: Periodic outbreaks of cholera, Poisson point process, Global stability, Bifurcation theory

1. Introduction

Cholera is an ancient waterborne disease caused by the bacterium *Vibrio cholerae* (*V. cholerea*), which is generally associated with poor sanitation and contaminated food and water supplies. Historically, seven cholera pandemics have been documented over the past 200 years. Recent severe epidemics of cholera took place in sub-Saharan Africa, south and south-east Asia and north America, including the outbreaks in Zimbabwe (2008-2009), Haiti (2010-2012) and Yemen (2016-2018). A number of epidemics and endemics of cholera have shown periodic patterns, which usually occurs annually or twice a year in endemic region and periods with various years for epidemic cycles (e.g., [Islam *et al.*, 2009; Wandiga *et al.*, 2006]). However, the mechanism behind the short-period endemic and long-period epidemic cycles is still poorly understood. A better understanding of the epidemic dynamics of cholera can improve the prevention and control of the

*Department of Mathematics and Statistics,Texas Tech University

future outbreaks. In this work, we focus on two biological factors, the host susceptibility and the virulence of *V. cholerea* in direct and indirect transmission routes, to study the disease dynamics, particularly, periodic outbreaks.

Human hosts can be infected by ingesting contaminated food/water or direct contact with infected human individuals. Patients may experience severe diarrhea [King *et al.*, 2008]. One determining factor is the dose of ingested bacteria. About 10^8 bacteria per milliliter are needed to cause severe cholera in healthy individuals [Sack *et al.*, 2004]. Host susceptibility is also closely associated with the immune system's ability. Patients with lowered immunity, such as children under malnutrition and HIV infected patients, are more likely to develop severe illness [Glass *et al.*, 1982]. Clinical studies show that 90% of patients with severe symptoms infected by the classical biotype can develop protective immunity against subsequent infection [Glass *et al.*, 1982]. Nevertheless, typically the antibody attributing to the protective immunity declines to the baseline after 6-9 months of the disease initiation [DiRita, 1995]. Oral cholera vaccines are available to provide sufficient protection in endemic regions [Organization, 2010]. Through bifurcation analysis, this paper demonstrates the influence of host responses on transmission rates and decay rates of protective immunity on disease outcomes, which aims to provide insight into the vaccination program in disease control.

The transmission of cholera involves direct transmission through human-to-human contacts (e.g., by shaking hands, or consuming foods prepared by infected people) [Merrell *et al.*, 2002; Morris Jr, 2011] and indirect transmission though environment-to-human contacts [Morris Jr, 2011]. A number of deterministic mathematical models have been proposed and analyzed to better understand the transmission dynamics of cholera (e.g., [Andrews & Basu, 2011; Capasso & Paveri-Fontana, 1979; Tien & Earn, 2010; Robertson *et al.*, 2013; Ghosh *et al.*, 2004; Tien *et al.*, 2010; Wang & Wang, 2015]). Most existing mathematical epidemic models are relatively simple autonomous ODE systems. The transmission incidences are often modeled by the standard mass-action law. If the number of susceptible and infected hosts are denoted as S and I, and the concentration of bacteria in the water environment is measured by B, the direct and indirect transmission incidence functions would be $\beta_H C_H IS$ and $\beta_E C_E BS$, respectively. Here β_H and β_E are total transmission rates for direct and indirect transmissions, respectively. Let C_H (resp. C_E) denote the probability of direct (resp. indirect) transmission occurring. Widely used incidence functions for this transmission route are the bilinear form with $C_H = p$ (for some $0 \leq p \leq 1$) [Tien & Earn, 2010; Robertson *et al.*, 2013; Ghosh *et al.*, 2004; Tien *et al.*, 2010] and a nonlinear form with $C_E \sim \frac{1}{B+\kappa_E}$ [Codeço, 2001; Mukandavire *et al.*, 2011; Tian *et al.*, 2013]. However, the corresponding autonomous ODE models usually can not capture the cyclical pattern in the cholera outbreak, as the endemic equilibrium is globally stable in the biological parameter space. Whereas, oscillations are often driven by some non-autonomous terms, such as a sinusoidal infection rate by exogenous force (such as seasonality). Investigating the intrinsic cause of the periodic outbreak of cholera is usually unavailable due to the lack of oscillation in most of the existing ODE models. In this paper, we formulate a simple nonlinear incidence function for the indirect transmission route base on a Poisson point process. The resulting autonomous cholera model is simple, but it can naturally generate regular and large-period oscillations, as a consequence of the rich behaviors of the underlying nonlinear system. Additionally, our results indicate that varying amplitudes and phases in annual or multi-annual cholera outbreaks can be further triggered by exogenous forces, such as seasonality.

The remainder of our paper is organized as follows. In Section 2, a nonlinear incidence function is derived through the Poisson point process to model the encounter between the pathogen and a host. This leads to a simple autonomous ODE model. In Section 3, we demonstrate dynamics of the proposed model, including analytical thresholds and conditions for the number of equilibriums and existence of backward and forward bifurcations. Global stability analysis on the disease-free equilibrium (DFE) and endemic equilibrium are presented in Section 4 through Lyapunov function and geometric approach, respectively. The parameter condition for the globally stable endemic equilibrium is very restricted. When this condition is violated, it results in rich dynamics. Section 5 explores complex disease dynamics through bifurcation analysis. More specifically, fold (static), Hopf and Bogdanov-Takens bifurcations are investigated. Two-parameter bifurcation diagrams are plotted to demonstrate outcomes of the disease in terms of parameter values. Annual and multi-annual outbreaks are numerically studied in Section 6. Further incorporating the exogenous seasonal force, the simulated outbreaks exhibit varying amplitudes and frequencies. A conclusion

is drawn in Section 7.

2. Model Derivation

2.1. *Formulation of Probability of Indirect Transmission Occurring*

This subsection focuses on the derivation of the indirect transmission probability, C_E, for the environmental-to-human transmission route. We assume that the human hosts are homogeneous. We first define:

(1) a: searching distance of a given pathogen;
(2) event: an encounter between the pathogen and a host;
(3) $X(a)$: total number of encounters ("events").

The number of host-pathogen encounters (HPEs) is assumed to be a stochastic process $\{X(a),\, a \geq 0\}$ in terms of the pathogen searching distance a, which satisfies the following properties:

(H1) $X(0) = 0$ a.s.;
(H2) for any $0 \leq a_1 < a_2 \leq a_3 < a_4$, $X(a_4) - X(a_3)$ is independent of $X(a_2) - X(a_1)$, where $X(a_2) - X(a_1)$ denotes the number of encounters occurred in the interval $(a_1,\, a_2]$;
(H3) $X(a_2 + d) - X(a_1 + d)$ has the same distribution as that of $X(a_2) - X(a_1)$, for any $0 \leq a_1 < a_2$, for all $d > 0$;
(H4)

$$\begin{aligned} &(i)\ \mathbb{P}(X(a + \Delta a) = 1 | X(a) = 0) = h(B)\, \Delta a + o(\Delta a); \\ &(ii)\ \mathbb{P}(X(a + \Delta a) \geq 2 | X(a) = 0) = o(\Delta a); \\ &\quad \text{where, } \mathbb{P} \text{ denotes probability.} \end{aligned}$$

Therefore, the total number of encounters $\{X(a),\, a \geq 0\}$ is a Poisson point process, which is continuous in searching distance a and discrete in the state space. (H1) indicates that no HPE occurs if pathogens do not move; (H2) indicates this process has the Markov property; (H3) ensures that this process has stationary increments in a sense the increment of encounters only depends on the length of the searching interval; (H4) assumes that the instantaneous transition rate of a new HPE per unit distance is given by $h(B) = b\frac{B}{B+K}$, where $b > 0$ is the searching probability of an individual pathogen per unit of distance, B measures the bacterial concentration in the water environment and K is the infectious dose in water sufficient to produce disease in 50% of those exposed. $h(B)$ describes the positive cooperation effect from peer pathogens on the pathogen of interest. For example, bacteria form biofilm to enhance resistance to environmental stresses [Silva & Benitez, 2016]. Therefore, we take $h(B)$ as an increasing and saturating function in the form of Michaelis–Menten equation.

By (H1)-(H4), $\{X(a)\}_{a \geq 0}$ is a simple birth-death process. It is known that

$$p_0(a) = \mathbb{P}\{X(a) = i\} = \mathbb{P}\{X(a) = 0 | X(0) = 0\} = e^{-ah(B)}. \tag{1}$$

A derivation of $p_0(a)$ is provided in Appendix A for self-completeness.

Moreover, what matters for HPEs is whether an encounter succeeds or not. The probability of having either no encounter between the pathogen and a host or at least one encounter are given by

$$\begin{aligned} &\mathbb{P}\{X(a) = 0\} = p_0(a) = e^{-ah(B)}, \\ &\mathbb{P}\{X(a) \geq 1\} = 1 - p_0(a) = 1 - e^{-ah(B)}, \end{aligned} \tag{2}$$

respectively. We assume the searching distance a follows an exponential distribution with parameter $\alpha_1 > 0$. The indirect transmission probability C_E is defined as the average encounter probability in terms of searching distance a, which is given by

$$C_E = \mathbb{E}\left[1 - p_0(a)\right] = 1 - \mathbb{E}\left[p_0(a)\right] = \frac{h(B)}{\alpha_1 + h(B)} = c_0 \frac{B}{B + K}, \tag{3}$$

where $\mathbb{E}$ denotes the expectation in term of random variable a, and $c_0 = \frac{1}{1+\alpha_1}$ and $K = \frac{\alpha_1 K_B}{1+\alpha_1}$. One may generalize $h(B)$ for instance $h(B) = \frac{B^p}{B^p + \alpha_p}$ for $p \geq 1$. The form in (3) is also justified in epidemiology [Pon-

Param.	Def.	Val.	Ref.
N	Total population size of humans	12347240 p	[Mukandavire *et al.*, 2011]
μ	Natural death rate of human	$1/(43.5 \times 365)\,\mathrm{d}^{-1}$	[WHO]
β_H	Direct transmission rate	estimated	
$\hat{\beta}_E$	Indirect transmission rate	$(0.25 \times 10^{-8}, 7 \times 10^{-8})$	[Mukandavire *et al.*, 2011]
K	Half saturation rate	$10^6\,\mathrm{cells} \cdot \mathrm{ml}^{-1}$	[Hartley *et al.*, 2005]
γ	Recovery rate	$0.2\,\mathrm{d}^{-1}$	[Hartley *et al.*, 2005]
σ	Rate of host immunity loss	$1/365\,\mathrm{d}^{-1}$	[Neilan *et al.*, 2010]
δ	Bacterial death rate	$0.23\,\mathrm{d}^{-1}$	[Hartley *et al.*, 2005]
ξ	Shedding rate	$10\,\mathrm{cells} \cdot \mathrm{ml}^{-1}\mathrm{p}^{-1}$	[Hartley *et al.*, 2005]

ciano & Capistrán, 2011] and ecological modeling, such as mating encounter [Dennis, 1989] and introducing sterile males in pest control [Costello & Taylor, 1975].

2.2. *A Cholera Model*

The dynamic model of cholera contains susceptible S, infected I and recovered R human population and the bacteria (vibrios) B in contaminated water. We assume that the probability of direct transmission occurring is $C_H = p$ for some $0 \le p \le 1$. By (3), the probability of in direct transmission occurring $C_E = c_0 B/(B + K)$. follows (3). Our new model takes the form

$$\begin{aligned} \frac{dS}{dt} &= \Lambda - \mu\, S - \beta_H\, I\, S - \beta_E\, \frac{B}{B+K}\, B\, S + \sigma\, R \\ \frac{dI}{dt} &= \beta_H\, I\, S + \beta_E\, \frac{B}{B+K}\, B\, S - (\mu + \gamma)\; I, \\ \frac{dR}{dt} &= \gamma I - (\mu + \sigma)\; R, \qquad \frac{dB}{dt} = \xi\, I - \delta\, B, \end{aligned} \tag{4}$$

where the parameter Λ is the recruitment rate of human hosts, and μ is the natural death rate of hosts. Infected individuals recover at a rate of γ, and wanes at a rate of σ. Upon the loss of the protective immunity, the recovered individuals join the susceptible group again. The inflow to the bacteria in contaminated water is only assumed from individuals, at the rate of ξ. Bacteria have a natural death rate δ. Direct and indirect total transmission rates are denoted as $\hat{\beta}_H$ and $\hat{\beta}_E$, respectively. For simplicity, we denote $\beta_H = \hat{\beta}_H p$ and $\beta_E = \hat{\beta}_E c_0$. The definition and the base values of the parameters are given in Table 1. The estimated ranges of β_H and β_E are provided in Appendix B.

3. Model analysis

3.1. *A biologically feasible region for solutions*

Let $N(t) = S(t) + I(t) + R(t)$ denote the total population size of hosts. Adding the first three equations of system (4) leads to $\frac{dN}{dt} = \Lambda - \mu N$. This implies that $N(t)$ is bounded, as

$$N(t) = N(0)e^{-\mu t} + S_0(1 - e^{-\mu t}) \le \max\{N(0), S_0\}, \quad \text{with } S_0 = \Lambda/\mu.$$

Meanwhile, if $B(0) \le \xi S_0/\delta$, then $B(t) \le \dfrac{\xi\, S_0}{\delta}$. Hence,

$$\Gamma = \left\{ (S,\, I,\, R,\, B) \in \mathbb{R}^4_+ \,\middle|\, S + I + R \le \max\{N(0), S_0\}, B \le \frac{\xi}{\delta}\, S_0 \right\}$$

gives us a biologically feasible region, which is positively invariant and bounded.

3.2. *Thresholds for Existence of Equilibriums and Backward Bifurcation*

Setting $\frac{dS}{dt} \triangleq f_1$, $\frac{dI}{dt} \triangleq f_2$, $\frac{dR}{dt} \triangleq f_3$, and $\frac{dB}{dt} \triangleq f_4$, equilibrium solutions of system (4) $E = (\bar{S}, \bar{I}, \bar{R}, \bar{B})$ are obtained by solving $f_1 = f_2 = f_3 = f_4 = 0$. Hence, we have

$$\bar{S} = \frac{\Lambda + \sigma\,\bar{R}}{\beta_E \dfrac{\bar{B}^2}{\bar{B} + K} + \beta_H\,\bar{I} + \mu}, \quad \bar{R} = \frac{\gamma\,\bar{I}}{\mu + \sigma}, \quad \bar{B} = \frac{\xi\,\bar{I}}{\delta}, \tag{5}$$

where $\bar{I}$ is the root of the following equation

$$\bar{I}\left(a_0\,\bar{I}^2 + a_1\,\bar{I} + a_2\right) = 0, \tag{6}$$

where

$$\begin{aligned}
a_0 &= (\beta_E\,\xi + \beta_H\,\delta)\,(\gamma\,+\,\mu\,+\,\sigma)\,\xi,\\
a_1 &= \frac{1}{\beta_H}\,\xi\,(\mu+\sigma)\,(\gamma\,+\,\mu)\,(\beta_E\,\xi\,+\,\beta_H\,\delta)\,\left(H\,-\,\frac{\beta_H\,S_0}{\gamma\,+\,\mu}\right),\\
a_2 &= (\gamma\,+\,\mu)\,(\mu\,+\,\sigma)\,\delta^2\,K\,\left(1 - \frac{\beta_H\,S_0}{\gamma\,+\,\mu}\right),\\
H &= \frac{\beta_H\,\delta}{\beta_E\,\xi\,+\,\beta_H\,\delta}\,+\,\frac{\beta_H^2\,\delta^2\,K\,(\gamma\,+\,\mu\,+\,\sigma)}{\xi\,(\mu\,+\,\sigma)\,(\gamma\,+\,\mu)\,(\beta_E\,\xi\,+\,\beta_H\,\delta)}.
\end{aligned} \tag{7}$$

Clearly, the trivial solution of (6), $\bar{I} = 0$, leads to a disease-free equilibrium (DFE) $E_0 = (S_0, 0, 0, 0)$ of system (6). The existence and number of endemic equilibriums depend on the following two thresholds in both direct and indirect transmission routes:

$$\beta_H = \frac{\mu\,+\,\gamma}{S_0} \triangleq \beta_{Ht}. \tag{8}$$

$$\beta_{Et} \triangleq \frac{(\mu+\gamma)\,(\gamma+\mu+\sigma)\,\delta^2\,K}{(\mu+\sigma)\,S_0^2\,\xi^2}. \tag{9}$$

Moreover, the preceding thresholds, β_{Ht} and β_{Et}, are two threshold values for the occurrence of transcritical and backward bifurcations.

Theorem 1 [Existence of equilibrium solutions]. *There exist at most three biologically feasible equilibria for model* (4) *which depend on values of* β_H *and* β_E. *The DFE* E_0 *always exists. Moreover, model* (4) *admits only one endemic equilibrium if either (a)* $\beta_H > \beta_{Ht}$ *or (b)* $\beta_H = \beta_{Ht}$ *and* $\beta_E > \beta_{Et}$ *holds; and two endemic equilibria coexist if* β_H *is sufficiently close to and smaller than* β_{Ht} *(that is,* $\beta_H \in (\beta_{Ht} - \beta_\epsilon,\, \beta_{Ht}) \in \mathbb{R}^+$*) and* $\beta_E > \beta_{Et}$.

Proof. Equation (6) has a trivial root $\bar{I} = 0$, which is the DFE for model (4). Positive roots of equation (6) can be derived from its second factor and if they exist, they take the form

$$I = \frac{-a_1 \pm \sqrt{\Delta}}{2\,a_0}, \quad \text{where} \quad \Delta = a_1^2 - 4\,a_0\,a_2, \tag{10}$$

where a_0, a_1, and a_2 are defined in (7). Since all parameters are positive, $a_0 > 0$. (i) If $a_2 < 0$ that is $\beta_H > \beta_{Ht} = \dfrac{\mu+\gamma}{N}$, equation (10) has only one positive root $I = \dfrac{-a_1 + \sqrt{a_1^2 - 4\,a_0\,a_2}}{2\,a_0}$ for all $a_1 \in \mathbb{R}$. (ii) If $a_2 = 0$ that is $\beta_H = \beta_{Ht}$, the only root $I = -\dfrac{a_1}{a_0}\Big|_{\beta_H=\beta_{Ht}}$ is positive if and only if $a_1|_{\beta_H=\beta_{Ht}} < 0$, which is equivalent to $\beta_E > \beta_{Et}$. (iii) If $a_2 > 0$ that is $\beta_H < \beta_{Ht}$, the existence of real roots requires $\Delta(\beta_H) \geq 0$. We notice that $\Delta|_{\beta_H=\beta_{Ht}} = (a_1|_{\beta_H=\beta_{Ht}})^2 > 0$. Since $\Delta(\beta_H)$ is a continuous function at $\beta_H = \beta_{Ht}$, there exists a value β_ϵ, such that for all $\beta_H \in (\beta_{Ht} - \beta_\epsilon,\, \beta_{Ht}) \in \mathbb{R}^+$, $\Delta(\beta_H) > 0$. Here, we omit the case where $\Delta|_{\beta_H=\beta_{Ht}} = 0$, since it implies $a_1|_{\beta_H=\beta_{Ht}} = a_2|_{\beta_H=\beta_{Ht}} = 0$, which yields a zero root. Thus two real roots

exist and take the form of (10), when $\Delta > 0$. Then the necessary condition for the positiveness of the two roots is

$$H_2 = \frac{\beta_H \delta}{\beta_E \xi + \beta_H \delta} + \frac{\beta_H \delta^2 K(\gamma + \mu + \sigma)}{\xi(\mu + \sigma)(\gamma + \mu)(\beta_E \xi + \delta \beta_H)} - \frac{S_0}{\gamma + \mu} < 0,$$

as

$$a_1 = \frac{1}{\beta_H} \xi (\mu + \sigma)(\gamma + \mu)(\beta_E \xi + \beta_H \delta) H_2, \quad \text{and } \operatorname{sign}(a_1) = \operatorname{sign}(H_2).$$

Since $H_2(\beta_H|\beta_E)$ is an increasing function, the necessary condition for $H_2(\beta_H|\beta_E) < 0$ when $\beta_H \in (0, \beta_{Ht})$ is $H_2(\beta_{Ht}|\beta_E) < 0$. Since $H_2\Big|_{\beta_H=\beta_{Ht},\, \beta_E=\beta_{Et}} = 0$ and H_2 is a decreasing function of β_E, $H_2(\beta_{Ht}|\beta_E) < 0$ implies $\beta_E > \beta_{Et}$. It follows from the continuity of H_2 in terms of β_H that the assertion about the coexisitence of endemic equilibria holds. ■

The local stability of the DFE is summarized in Lemma 1. Conditions for backward and forward bifurcations are derived by applying Theorem 2 in [van den Driessche & Watmough, 2002].

Lemma 1. *The DFE* $E_0 = (\Lambda/\mu, 0, 0, 0)$ *is locally asymptotically stable in* Γ *if* $\beta_H < \beta_{Ht}$ *and unstable if* $\beta_H > \beta_{Ht}$.

Proof. See Theorem 2. ■

Theorem 2 [Conditions of backward and forward bifurcations]. *System* (4) *undergoes a transcritical bifurcation at* $\beta_H = \beta_{Ht}$, *which further induces a backward bifurcation if* $\beta_E > \beta_{Et}$ *and a forward bifurcation if* $\beta_E < \beta_{Et}$.

Proof. The theorem is proved by the center manifold of the DFE E_0 at one zero eigenvalue point. Here, parameters β_H and β_E are set as bifurcation and control parameters. First, we evaluate the Jacobian matrix of (4) at the DFE E_0 and obtain the corresponding characteristic polynomial $q_0(x)$:

$$q_0(L) = (L + \mu)(L + \mu + \sigma)(L + \delta)(L - S_0 \beta_H + \gamma + \mu).$$

The roots of $q_0(L) = 0$ give the eigenvalues of the DFE E_0, which include three negative ones. The single zero eigenvalue happens when $-S_0 \beta_H + \gamma + \mu = 0$ or $\beta_H = \beta_{Ht}$ in (8). At this point, the DFE E_0 becomes non-hyperbolic equilibrium, whose stability can not be determined by the linear analysis. Next, we project the three dimensional stable manifold into the center manifold to study the local dynamics of the DFE E_0. The derivation follows the result of the Theorem 4.1 by [Castillo-Chavez & Song, 2004]. The time-dependent function associated with the center manifold of the DFE E_0 at $\beta_H = \beta_{Ht}$ is denoted by $c(t)$. The expression of its vector field up to the second order can be written as

$$\frac{dc}{dt} = \frac{a}{2} c^2 + b\phi c, \quad a = \sum_{k,i,j=1}^{4} v_k w_i w_j \frac{\partial^2 f_k}{\partial x_i \partial x_j}(\vec{x}, \phi)\Big|_{(\vec{0},0)}, \quad b = \sum_{k,i=1}^{4} v_k w_i \frac{\partial^2 f_k}{\partial x_i \partial \phi}(\vec{x}, \phi)\Big|_{(\vec{0},0)}, \tag{11}$$

where $\phi = \beta_H - \beta_{Ht}$ is the new bifurcation parameter, $\vec{x} = (x_1, x_2, x_3, x_4)^T \triangleq (S, I, R, B)^T$, $(f_1, f_2, f_3, f_4)^T = (\frac{dS}{dt}, \frac{dI}{dt}, \frac{dR}{dt}, \frac{dR}{dt})^T$. The DFE E_0 is shifted to $\vec{x} = \vec{0}$. The corresponding Jacobian matrix evaluated at E_0 is denoted as $D_x f(\vec{0}, \phi) = \left[\frac{\partial f_k}{\partial x_i}\right]\Big|_{\vec{x}=\vec{0}}$, which admits a zero eigenvalue at $\phi = \beta_H - \beta_{Ht} = 0$. Then

$$D_x f(\vec{0}, 0) = \begin{bmatrix} -\mu & -(\mu + \gamma) & \sigma & 0 \\ 0 & 0 & 0 & 0 \\ 0 & \gamma & -(\mu + \sigma) & 0 \\ 0 & \xi & 0 & -\delta \end{bmatrix}.$$

Obviously, $D_x f(\vec{0}, 0)$ has a simple zero eigenvalue with the right eigenvector

$$\vec{w} = \left[-\frac{\gamma + \mu + \sigma}{\gamma},\, \frac{\mu + \sigma}{\gamma},\, 1,\, \frac{\xi\,(\mu + \sigma)}{\gamma\,\delta} \right]^T,$$

and the left eigenvector

$$\vec{v} = \left[0,\, \frac{\gamma}{\mu + \sigma},\, 0,\, 0 \right]^T$$

such that $\vec{v} \cdot \vec{w} = 1$. Hessian matrices $D_{xx} f(\vec{0}, 0)$ and $D_{x\phi} f(\vec{0}, 0)$ have nonzero elements as follows

$$\frac{\partial^2 f_1}{\partial x_1 x_2}(\vec{0},\, 0) = \frac{\partial^2 f_1}{\partial x_2 x_1}(\vec{0},\, 0) = -\frac{\partial^2 f_2}{\partial x_1 x_2}(\vec{0},\, 0) = -\frac{\partial^2 f_2}{\partial x_2 x_1}(\vec{0},\, 0) = -\beta_{Ht} = -\frac{\mu + \gamma}{S_0},$$
$$\frac{\partial^2 f_1}{\partial x_4^2}(\vec{0},\, 0) = -\frac{\partial^2 f_2}{\partial x_4^2}(\vec{0},\, 0) = -\frac{2\beta_E S_0}{K},\ \text{and}\ \frac{\partial^2 f_1}{\partial x_2 \phi}(\vec{0},\, 0) = -\frac{\partial^2 f_2}{\partial x_2 \phi}(\vec{0},\, 0) = -S_0,$$

which yield

$$a = -\frac{(\gamma + \mu + \sigma)(\mu + \gamma)}{\gamma S_0} + \frac{(\mu + \sigma)\xi^2 \beta_E S_0}{\gamma \delta^2 K} = \frac{(\gamma + \mu + \sigma)(\mu + \gamma)}{\gamma S_0} \left(\frac{\beta_E}{\beta_{Et}} - 1 \right), \quad b = S_0. \tag{12}$$

The orbit structure of system (4) near the DFE E_0 at $\beta_H = \beta_{Ht}$ is qualitatively the same as the orbit structure of the first of equation in (11) near $(c,\, \phi) = (0,\, 0)$. Moreover, the first equation in (11) takes a normal form for the transcritical bifurcation. Since $b > 0$ in (12), forward bifurcation happens if $a < 0$ ($\beta_E < \beta_{Et}$), and backward bifurcation occurs if $a > 0$ ($\beta_E > \beta_{Et}$). ■

4. Global Stability of Equilibrium Solutions

In view of the existence of a backward bifurcation in model (4), we analyze for the global stability of the DFE and the endemic equilibrium.

4.1. *Analysis via Lyapunov Function*

Theorem 3. *If $\beta_H < \beta_{Ht}\, G$, the DFE E_0 of (4) is globally asymptotically stable in Γ, where*

$$G \triangleq 1 - \frac{\beta_E\, S_0\, \xi}{\delta\,(\mu + \gamma)}. \tag{13}$$

Proof. We only need to consider solutions of system (4) in the bounded positive invariant set Γ, that is $(S(t),\, I(t),\, R(t),\, B(t)) \in \Gamma$. Then we have the following two inequalities

$$0 \le \frac{B}{B + K} \le 1, \qquad 0 \le S \le S_0. \tag{14}$$

Considering $V(t) = \delta\, I(t) + \beta_E\, S_0\, B(t)$ as a Lyapunov function along the solution of (4) in Γ, we have

$$\begin{aligned} \frac{dV}{dt} &= \delta\, \frac{dI}{dt} + \beta_E\, S_0\, \frac{dB}{dt} \\ &= \delta\, \beta_H\, I\, S + \delta\, \beta_E\, B\, S - \delta\,(\mu + \gamma)\, I + \beta_E\, S_0\, \xi\, I - \beta_E\, S_0\, \delta\, B \\ &\le \delta\, \beta_H\, I\, S_0 - \delta(\mu + \gamma)\, I + \beta_E\, S_0\, \xi I \\ &= \delta I(\mu + \gamma) \left[\frac{\beta_H\, S_0}{\mu + \gamma} + \frac{\beta_E\, S_0\, \xi}{\delta\,(\mu + \gamma)} - 1 \right] \\ &= \delta I(\mu + \gamma) \left(\frac{\beta_H}{\beta_{Ht}} - G \right) \le 0,\ \text{if}\ \beta_H < \beta_{Ht}\, G, \end{aligned} \tag{15}$$

by applying two inequalities in (14). If $\frac{dV}{dt} = 0$ then $I = 0$ as $\beta_H < \beta_{Ht} G$. We define $\Lambda = \left\{(S, I, R, B) \in \Gamma | \frac{dV}{dt} = 0\right\} \subseteq \{(S, I, R, B) \in \Gamma | I = 0\}$. Since $V(t)$ decreases along a solution of system (4) according to (15), the omega-limit set of the solution is contained in the set Λ. The omega-limit set is also contained in the largest invariant subset K, since it is invariant. A solution stays in Λ satisfies $\lim_{t\to+\infty} I(t) = \lim_{t\to+\infty} B(t) = 0$, which follows with $\lim_{t\to+\infty} R(t) = 0$ and $\lim_{t\to+\infty} S(t) = S_0$. Hence, the largest invariant subset $K = \{E_0\}$. Therefore, the global asymptotic stability of E_0 follow from LaSalle's Invariance Principle [Li, 2018] when $\beta_H < \beta_{Ht} G$. ■

Biologically, Theorem 3 provides a sufficient condition for cholera elimination; that is

$$R_2 \triangleq \frac{\beta_H S_0}{\mu + \gamma} + \frac{\beta_E S_0}{\mu + \gamma} \frac{\xi}{\delta} < 1. \tag{16}$$

The preceding threshold indicates that an infected individual can produce $\beta_H \cdot S_0 \cdot \frac{1}{\mu+\gamma}$ (resp. $\beta_E \cdot S_0 \cdot \frac{1}{\mu+\gamma} \cdot \frac{\xi}{\delta}$) secondary infection through direct (resp. indirect) transmission on average.

4.2. *Global Stability Analysis by Geometric Method*

Li and Muldowney developed a geometric approach [Li & Muldowney, 1995, 1996], which generalizes the Bendixson criterion for 2-dimensional ODE model and provides an approach to derive a global-stability result for a general nonlinear ODE system. This geometric approach is widely applied to ecological models (e.g., [Ballyk *et al.*, 2005; Lu & Lu, 2012]) and infectious disease models (e.g., [Smith *et al.*, 2001; Arino *et al.*, 2003; Feng *et al.*, 2015; Lu & Lu, 2017]).

In this subsection, we employ the geometric approach based on the second additive compound matrix [Muldowney, 1990; Li & Muldowney, 1995] to analyse the endemic global stability of our model. A brief summary of this technique is provided in Appendix C.

Proposition 1. *If $\beta_H > \beta_{Ht}$, the system* (4)*is uniformly persistent in the interior of* Γ.

Proof. By Theorem 1, model (4) always admits the DFE E_0 Moreover, E_0 is unstable when $\beta_H > \beta_{Ht}$. Combine with Theorem 4.3 from [Freedman *et al.*, 1994], the instability of E_0 is equivalent to the uniform persistence of model (4) in the interior of Γ. ■

Proposition 1 implies that there exists $c > 0$ such that $\forall\, x_0 \in \bar{\Gamma}$, the solution $x(t, x_0)$ of system (4) satisfies $\liminf_{t\to\infty} \mathrm{d}(x(t, x_0), \partial\Gamma) > c$, where $\mathrm{d}(\cdot, \cdot)$ denotes the Euclidean distance. Biologically, this result implies uniform persistence of the disease, since the infected population $I(t)$ and the bacterium population $B(t)$ will stay above a positive level c for all sufficiently large time. By the boundedness of Γ, the uniform persistence of model (4) implies the existence of a compact absorbing set $K \subset \bar{\Gamma}$. Furthermore, by assuming K is the largest compact absorbing set, each compact set $K_0 \subset \bar{\Gamma}$ satisfies the omega limit set $\omega(K_0) \subset K$ [Li & Muldowney, 1996; Smith *et al.*, 2001]. By Theorem 1, the endemic equilibrium E_1 is unique in $\bar{\Gamma}$ when $\beta_H > \beta_{Ht}$. Therefore, the assumptions in Theorem 5 are valid. Next, we find the condition for the inequality (43) to be satisfied when $\beta_H > \beta_{Ht}$.

The Jacobian matrix $J = \frac{\partial f}{\partial x}$ and its corresponding second compound matrix $J^{[2]} = \frac{\partial f}{\partial x}^{[2]}$ [Li & Muldowney, 1995] can be calculated as follows:

$$J = \begin{bmatrix} -\frac{B^2\beta_E}{B+K} - \beta_H I - \mu & -\beta_H S & \sigma & -J_2 \\ \beta_H I + \frac{B^2\beta_E}{B+K} & \beta_H S - \gamma - \mu & 0 & J_2 \\ 0 & \gamma & -\mu - \sigma & 0 \\ 0 & \xi & 0 & -\delta \end{bmatrix}$$

and

$$J^{[2]} = \begin{bmatrix} J_1 & 0 & J_2 & -\sigma & J_2 & 0 \\ \gamma & J_3 & 0 & -\beta_H S & 0 & J_2 \\ \xi & 0 & J_4 & 0 & -\beta_H S & \sigma \\ 0 & J_5 & 0 & J_6 & 0 & -J_2 \\ 0 & 0 & J_5 & 0 & J_7 & 0 \\ 0 & 0 & 0 & -\xi & \gamma & J_8 \end{bmatrix},$$

where,

$$\begin{aligned} J_1 &= -\tfrac{B^2\beta_E}{B+K} + (S-I)\beta_H - 2\mu - \gamma, \; J_2 = \tfrac{\beta_E SB(B+2K)}{(B+K)^2}, \\ J_3 &= -\tfrac{B^2\beta_E}{B+K} - \beta_H I - 2\mu - \sigma, & J_4 &= -\tfrac{\beta_E B^2}{B+K} - \beta_H I - \delta - \mu, \\ J_5 &= \beta_H I + \tfrac{\beta_E B^2}{B+K}, & J_6 &= \beta_H S - \gamma - 2\mu - \sigma, \\ J_7 &= \beta_H S - \delta - \gamma - \mu, & J_8 &= -\mu - \sigma - \delta. \end{aligned}$$

We set $A = (a_{ij})$ as a 6×6 matrix, whose nonzero elements are $a_{11} = a_{22} = a_{34} = 1/I$ and $a_{43} = a_{55} = a_{66} = 2/B$. Setting $f = (\frac{dS}{dt}\ \frac{dI}{dt}\ \frac{dR}{dt}\ \frac{dB}{dt})$, the matrix

$$\mathcal{B} = A_f A^{-1} + A\frac{\partial f}{\partial x}^{[2]} A^{-1} \tag{17}$$

can be written in the following block form:

$$\mathcal{B} = \begin{bmatrix} B_{11} & B_{12} & B_{13} & 0 \\ B_{21} & B_{22} & \mathbf{0} & B_{24} \\ B_{31} & \mathbf{0} & B_{33} & B_{34} \\ 0 & B_{42} & B_{43} & B_{44} \end{bmatrix}$$

where,

$$B_{11} = -\beta_H I - \mu - \tfrac{\beta_E B^2}{B+K} - \tfrac{\beta_E SB^2}{I(B+K)}, \qquad B_{12} = [0\ -\sigma], \qquad B_{13} = \left[\tfrac{BJ_2}{I}\ \tfrac{BJ_2}{I}\right],$$

$$B_{21} = \begin{bmatrix} \gamma \\ 0 \end{bmatrix}, \quad B_{22} = \begin{bmatrix} -\beta_H I - \beta_H S + \gamma - \mu - \sigma - \tfrac{\beta_E B^2}{B+K}(1+\tfrac{S}{I}) & -\beta_H S \\ J_5 & -\mu - \sigma - \tfrac{\beta_E SB^2}{I(B+K)} \end{bmatrix}, \quad B_{24} = \begin{bmatrix} \frac{BJ_2}{I} \\ \frac{BJ_2}{I} \end{bmatrix},$$

$$B_{31} = \begin{bmatrix} \frac{\xi I}{B} \\ 0 \end{bmatrix}, \quad B_{33} = \begin{bmatrix} -\frac{\beta_E B^2}{B+K} - (\beta_H I + \mu)\frac{B}{B+K} - \frac{(K\beta_H+\xi)I + \mu K + K\xi I}{B(B+K)} & -\beta_H S \\ J_5 & \beta_H S - \gamma - \mu - \frac{\xi I}{B} \end{bmatrix}, \quad B_{34} = \begin{bmatrix} \sigma \\ 0 \end{bmatrix},$$

$$B_{42} = \left[0\ -\tfrac{\xi I}{B}\right], \qquad B_{43} = \left[0\ \gamma\right], \qquad B_{44} = -\mu - \sigma - \tfrac{\xi I}{B}.$$

We choose the vector norm in $\mathbb{R}^4 \cong \mathbb{R}^{\binom{4}{2}}$ as

$$|\ (v_1, v_2, v_3, v_4, v_5, v_6)\ | = \max\{|\ v_1\ |, |\ v_2 + v_3\ |, |\ v_4 + v_5\ |, |\ v_6\ |\}.$$

The Lozinski$\breve{i}$ measure, $M(\mathcal{B}) = \max_i \left(B_{ii} + \sum_{j\neq i} |B_{ij}|\right)$, with respect to the above defined vector norm has the following relation [Martin Jr, 1974; Muldowney, 1984]:

$$M(\mathcal{B}) \leq \max\{g_1,\, g_2,\, g_3,\, g_4\}.$$

Following the formula $g_i = M(B_{ii}) + \sum_{j\neq i} |B_{ij}|$, we have

$$\begin{aligned} g_1 &= B_{11} + |B_{12}| + |B_{13}| = -\beta_H I - \mu + \sigma - \tfrac{\beta_E B^2}{B+K} - \tfrac{\beta_E SB^3}{2I(B+K)^2} < -\mu + \sigma = -\mu + b_1; \\ g_4 &= B_{44} + |B_{42}| + |B_{43}| = -\mu - \sigma + \gamma + \tfrac{\xi I}{B} = -\mu + b_4 + \tfrac{\dot{B}}{B}; \end{aligned}$$

If $-2\left(\beta_H I + \frac{\beta_E B}{B+K}\right) + \gamma \geq 0$, then $M(B_{22}) = (B_{22})_{(1,1)} + |(B_{22})_{(1,2)}|$ and hence

$$\begin{aligned} g_2 &= (B_{22})_{(1,1)} + |(B_{22})_{(1,2)}| + |B_{21}| + |B_{24}| = -\beta_H I - \tfrac{\beta_E B^2}{B+K} - \mu - \sigma + 2\gamma - \tfrac{\beta_E S B^3}{2I(B+K)^2} \\ &< -\mu - \sigma + 2\gamma = -\mu + b_2, \\ g_3 &= (B_{33})_{(1,1)} + |(B_{33})_{(1,2)}| + |B_{31}| + |B_{34}| = -\tfrac{\beta_E B^2}{B+K} - \beta_H I + \beta_H S - \mu + \sigma + \tfrac{\xi I}{B+K} + \tfrac{\xi K I}{B(B+K)} \\ &< \beta_H S - \mu + \sigma + \tfrac{\xi I}{B} < \beta_H S_0(1+\tfrac{\xi}{\sigma}) - \mu + \sigma + \delta + \tfrac{\dot{B}}{B} = -\mu + b_3 + \tfrac{\dot{B}}{B}. \end{aligned}$$

If $-2\left(\beta_H I + \frac{\beta_E B}{B+K}\right) + \gamma < 0$, then $M(B_{22}) = (B_{22})_{(2,2)} + |(B_{22})_{(2,1)}|$ and in this case,

$$\begin{aligned} g_2 &= (B_{22})_{(2,2)} + |(B_{22})_{(2,1)}| + |B_{21}| + |B_{24}| = \beta_H I + \tfrac{\beta_E B^2}{B+K} - \mu - \sigma + \gamma - \tfrac{\beta_E S B^2}{I(B+K)} + \tfrac{\beta_E S B^2 (K+B/2)}{I(B+K)^2} \\ &< \beta_H I + \beta_E B - \mu - \sigma + \gamma < (\beta_H + \beta_E) S_0 (1+\tfrac{\xi}{\sigma}) + \gamma - \mu - \sigma = -\mu + \tilde{b}_2, \\ g_3 &= \tfrac{\beta_E B^2}{B+K} + \beta_H (S+I) - \gamma - \mu - \tfrac{\xi I}{B} + \sigma + \tfrac{\xi I}{B} < (2\beta_H + \beta_E) S_0 (1+\tfrac{\xi}{\delta}) - \gamma - \mu + \sigma = -\mu + \tilde{b}_3; \end{aligned}$$

where,

$$\begin{aligned} & b_1 = \sigma, \quad b_2 = 2\gamma - \sigma, \quad \tilde{b}_2 = (\beta_H + \beta_E) S_0 (1+\tfrac{\xi}{\sigma}) + \gamma - \sigma \\ & b_3 = \beta_H S_0 (1+\tfrac{\xi}{\sigma}) + \sigma + \delta, \quad \tilde{b}_3 = (2\beta_H + \beta_E) S_0 (1+\tfrac{\xi}{\delta}) - \gamma + \sigma, \quad b_4 = \gamma - \sigma < b_2. \end{aligned}$$

We choose

$$b = \max\{b_1,\, b_2,\, \tilde{b}_2,\, b_3,\, \tilde{b}_3\}, \tag{18}$$

then have

$$g_1 < -\mu + b, \quad g_2 < -\mu + b, \quad g_3 < -\mu + b + \frac{\dot{B}}{B}, \quad g_4 < -\mu + b + \frac{\dot{B}}{B},$$

and

$$M(\mathcal{B}) < \max\{g_1,\, g_2,\, g_3,\, g_4\} < -\mu + b + \frac{\dot{B}}{B}.$$

Along each solution $x(t, x_0)$, for $x_0 \in \Gamma$ and $t > T > 0$, we have

$$\frac{1}{t}\int_0^t M(\mathcal{B}) ds < \frac{1}{t}\int_0^T M(\mathcal{B}) ds + \frac{1}{t}\ln\frac{B(t)}{B(T)} - (\mu - b)\frac{t-T}{t},$$

and

$$\bar{q} = \limsup_{t\to\infty} \sup_{x_0\in\Gamma} \frac{1}{t}\int_0^t M[\mathcal{B}(x(s,x_0))] ds < \limsup_{t\to\infty} \sup_{x_0\in\Gamma} (-b\frac{t-T}{t}) \leq -(\mu - b) < 0, \text{ if } \mu > b.$$

A Bendixson criterion $\bar{q} < 0$ [Li & Muldowney, 1995] is verified and followed the global stability result for endemic equilibrium E_1:

Theorem 4. *If $\beta_H > \beta_{Ht}$ and $\mu > b$ in* (18)*, the system* (4) *is globally asymptotically stable.*

Theorem 4 provides a strong condition for the global stability of the endemic equilibrium.

5. Bifurcation Analysis on the Endemic Equilibrium

Although the global stability analysis of the DFE and the endemic equilibrium (Theorems 3-4) provides some useful information on disease dynamics, it only covers some extremely cases. We now apply the bifurcation theory to further investigate the disease dynamics. Our concern is the influence of two transmission routes, environmental bacteria surviving and host immune response to the disease on the disease dynamics. We, therefore, focus on direct and indirect transmission rates (β_H and β_E), host recovery rate (γ), host immunity losing rate (σ), and bacteria death rate (δ).

The changing rates of S, I and R are much more slower than that of B (e.g., humans have longer life span than bacteria). Model (4) is a stiff system, which usually cause inefficiency or even failure of numerical solvers. So we first do appropriate scaling, and then analyze stiff systems by using bifurcation theory and numerical bifurcation methods [Yu, 2005, 1998].

5.1. *Bifurcation Diagrams*

First, we use bifurcation diagrams to categorize the dynamical behaviors of our model. Write model (4) as

$$\frac{dx}{dt} = f(x, \alpha), \quad x = (S, I, R, B) \in \mathbb{R}^4_+, \quad \alpha = (\beta_H, \beta_E) \in \mathbb{R}^2_+, \tag{19}$$

where the other fixed parameter values are taken from Table (1). Suppose that at $\alpha = \alpha_0$, system (19) has a positive equilibrium $x_E = (\bar{S}, \bar{I}, \bar{R}, \bar{B})$ in (5). Then bifurcation conditions for x_E at $\alpha = \alpha_0$ give bifurcation diagrams in the (β_H, β_E) plane, along which the system shows corresponding bifurcations. To avoid the complexity involved in model dimension and parameter values, we derive closed-form expressions of bifurcation conditions for system (19) by using the results from [Yu, 2005]. First, we evaluate the Jocobian matrix of system (19) at a equilibrium $x_E = x_E(\alpha)$, which yields $J(\alpha) = Df|_{x=x_E(\alpha)}$. Then the corresponding characteristic polynomial is given as

$$P_4(\lambda) = \det[\lambda I - J(\alpha)] = \lambda^4 + c_1(\alpha)\,\lambda^3 + c_2(\alpha)\,\lambda^2 + c_3(\alpha)\,\lambda + c_4(\alpha), \tag{20}$$

and the corresponding Hurwitz arrangements

$$\Delta_1 = c_1,\ \Delta_2 = c_1c_2 - c_3,\ \Delta_3 = (c_1c_2 - c_3)c_3 - c_1^2c_4,\ \Delta_4 = (c_1c_2 - c_3)c_3c_4 - c_1^2c_4^2. \tag{21}$$

According to the Theorems 1 and 2 from [Yu, 2005], we have that the necessary and sufficient condition for the system (19) to exhibit

(1) a static bifurcation, if $c_4 = 0$ and $\Delta_i > 0$ for $i = 1, 2, 3$;
(2) a Bogdanov-Takens bifurcation, if $c_4 = c_3 = 0$ and $c_i > 0$ for $i = 1, 2$;
(3) a Hopf bifurcation, if $\Delta_3 = 0$, $\Delta_i > 0$ for $i = 1, 2$ and $c_4 > 0$;

The results are summarized in bifurcation diagrams Figures 2 and 1. In these figures, "T", "SN", and "H" denote transcritical, saddle-Node, and Hopf bifurcation curves, respectively. 2-dimensional bifurcation diagrams in terms of δ-β_H, γ-β_H, σ-β_H, γ-σ, and β_E-β_H are plotted. Model (4) exhibits one, three, and two equilibrium solutions displayed in green, yellow and red parameter regions, respectively, which are delimited by saddle-node and transcritical bifurcation curves. Hopf bifurcation is a source for oscillation, which will be further investigated.

Biologically, green, yellow, and red parameter regions in 2-dimensional bifurcation diagrams indicate the model behavior representing disease elimination, dose-dependent effects, and periodic outbreaks, respectively. To eliminate the disease, efforts should be made in increasing bacteria decay rate (δ) and host recovery rate (γ), but reducing the two transmission rates (β_E and β_H). Since the condition of transcritical bifurcation (8) does not involve δ, β_H, or γ, the transcritical bifurcation curves in Figure 1 (a), (b), and (c) are independent of the bacteria decay rate, environment-human transmission rate, and host recovery rate. Notice that colliding points between saddle-node and transcritical curves in sub-figures (a), (c), and (d) serve as thresholds for backward bifurcations. The increase in host immunity loss rate σ can lead to backward bifurcation, which can trigger the bi-stability in cholera epidemic dynamics (see yellow region in Figures 1 c).

Next, we focus on infection rates corresponding to two transmission routes to investigate the oscillations due to Hopf bifurcations. Taken three values of parameter β_E, the corresponding 1-dimensional bifurcation diagrams are shown in sub-figures (b), (c), and (d). The bifurcation critical points in Figure 2 are

(1) Transcritical bifurcation: $x_E = (1.234724 \times 10^7, 0, 0, 0)$ and $\beta_H = 0.16203 \times 10^{-7}$ for all three β_E values in sub-figures (b), (c), and (d);
(2) Saddle-Node bifurcation: $x_E = (9.847801 \times 10^6, 34542, 2.464896 \times 10^6, 0.1480368 \times 10^7)$, $\beta_H = 7.5261 \times 10^{-7}$ for the sub-figure (b); $x_E = (8.082416 \times 10^6, 58939, 4.205884 \times 10^6, 2.525971 \times$

10^6), $\beta_H = -2.13007 \times 10^{-8}$ for the sub-figure (c); $x_E = (7.194440 \times 10^6, 71211, 5.081588 \times 10^6, 3.051902 \times 10^6)$, $\beta_H = 5.289225 \times 10^{-8}$ for the sub-figure (d);

(3) Hopf bifurcation: $x_E = (3.810309 \times 10^6, 117979, 8.418951 \times 10^6, 5.056256 \times 10^6)$, $\beta_H = 3.4615 \times 10^{-8}$ and the first focus value $v_1 = 2.191 \times 10^{-17}$ for the sub-figure (b); $x_E = (2.443584 \times 10^6, 136867, 9.766789 \times 10^6, 5.865741 \times 10^6)$, $\beta_H = 2.69503 \times 10^{-8}$ and the first focus value $v_1 = 2.851 \times 10^{-17}$ for the sub-figure (c); $x_E = (1.975475 \times 10^7, 143336, 1.0228428 \times 10^6, 6.1429927 \times 10^6)$, $\beta_H = 9.1302 \times 10^{-9}$ the first focus value $v_1 = 4.433 \times 10^{-17}$ for the sub-figure (d).

Therefore, Hopf bifurcations in these three cases are all subcritical and generate unstable limit cycles. Other than a small parameter region in case (d),the DFE is unstable. It indicates the existence of a stable attractor between the bifurcated unstable limit cycle and the unstable DFE. This prediction is proved to be true in the next subsection.

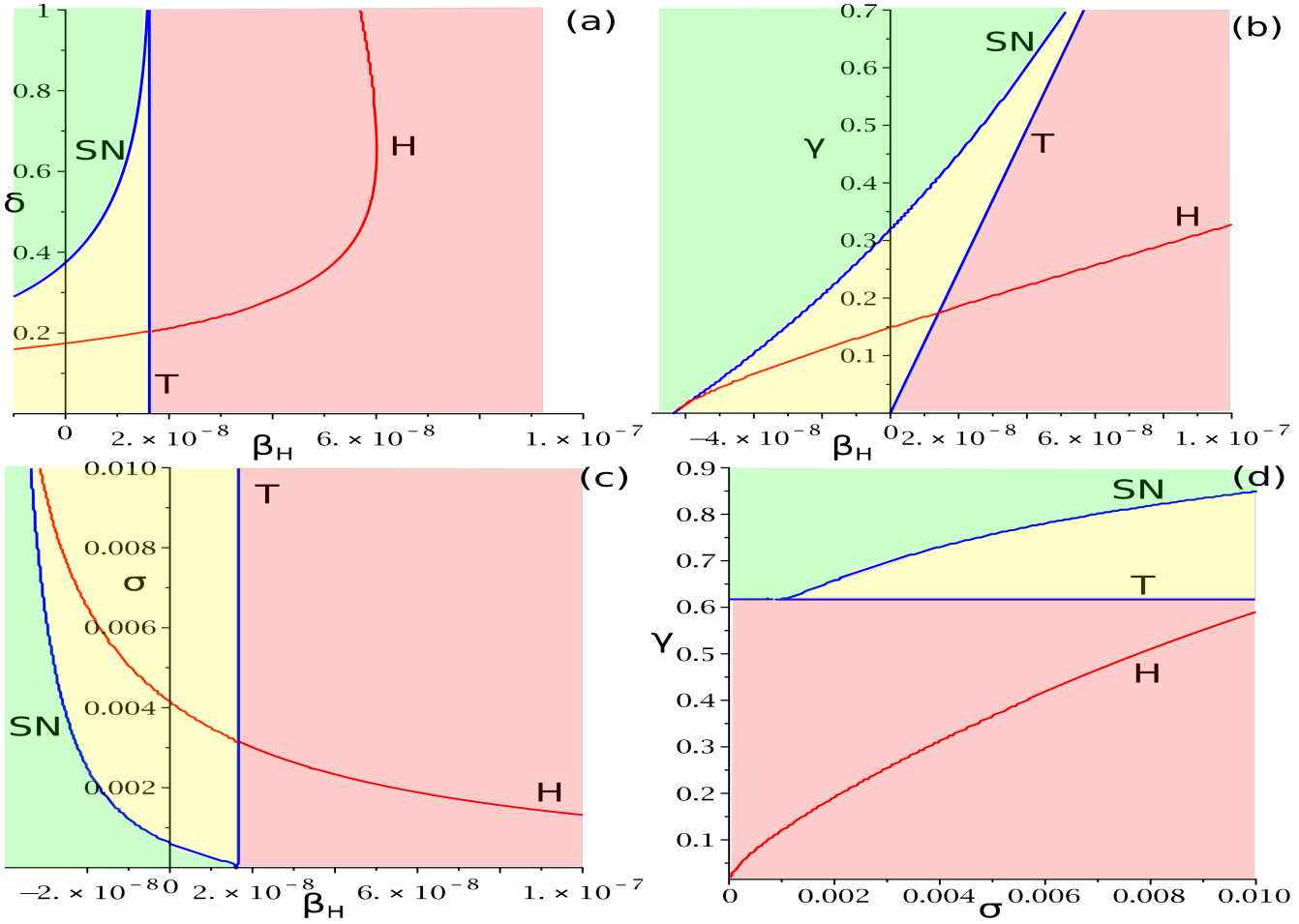

Fig. 1. Two-parameter bifurcation diagrams in terms of the bacteria decay rate (δ), host recovery rate (γ), host immunity loss (σ), and direct transmission rate (β_H).

5.2. *Computation of a normal form to a Hopf bifurcation*

Chosen $\beta_E = 2.5 \times 10^{-9}$, system (4) exhibits a Hopf bifurcation at

$$x_E^0 = (1.975475 \times 10^6, 143336, 1.0228428 \times 10^6, 6.1429927 \times 10^6), \quad \beta_H^0 = 9.1302 \times 10^{-8}.$$

We then choose this critical point to carry out a Hopf bifurcation analysis. First, we introduce the following parameter transformation

$$\beta_H = \beta_H^0 + \epsilon, \tag{22}$$

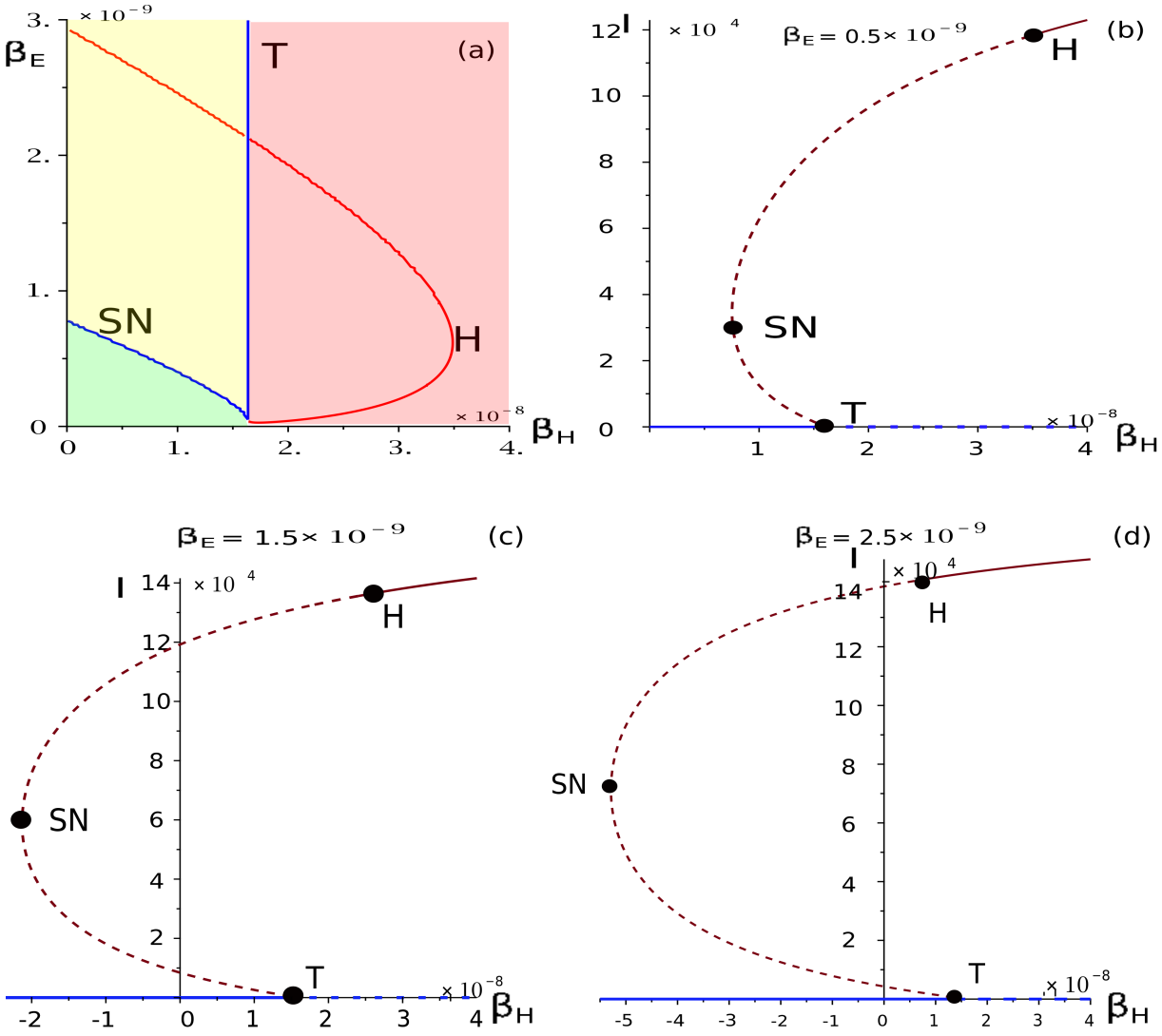

Fig. 2. Bifurcation diagrams of model (4). (a) A two-parameter bifurcation in terms of two infection rates β_E and β_H. (b)-(d) displays bifurcation diagrams of I as a function of β_H with varied β_E. Here DFE and endemic equilibriums are in blue and red, respectively. Stable and unstable equilibrium solutions are denoted in solid and dashed curves, respectively.

where ϵ the bifurcation parameter. The corresponding equilibrium is $\bar{x}_E = (S(\epsilon), I(\epsilon), R(\epsilon), B(\epsilon))$, with

$$\begin{aligned} S(\epsilon) &= 1975475.4681 - 19991382557872.0476\epsilon, \\ I(\epsilon) &= 143336.4974 + 276278423548.2317\epsilon, \\ R(\epsilon) &= 10228428.0344 + 19715104134323.8159\epsilon, \\ B(\epsilon) &= 6142992.7462 + 11840503866352.7877\epsilon. \end{aligned} \tag{23}$$

Introduce the state variable transformation

$$x = \bar{x}_E + T_1 Z, \tag{24}$$

where $z \in \mathbb{R}^4_+$ and T_1 as follows,

$$T_1 = \begin{bmatrix} -5.0868 \times 10^{-2} & 0.11095 & 2.0827 \times 10^{-2} & 1.0657 \times 10^{-2} \\ 2.2988 \times 10^{-2} & 3.8775 \times 10^{-3} & -1.1809 \times 10^{-2} & 1.9928 \times 10^{-2} \\ 2.7881 \times 10^{-2} & -0.11483 & -0.86206 & -9.2718 \times 10^{-3} \\ 0.98519 & 0 & -0.506239 & -0.99970 \end{bmatrix}. \tag{25}$$

Then the system (4) is transformed into a new system

$$\frac{dz}{dt} = J_1 z + H_1(Z;\, \epsilon), \tag{26}$$

where J_1 in Jordan canonical form

$$J_1 = \begin{bmatrix} 0 & 0.039358 & 0 & 0 \\ -0.039358 & 0 & 0 & 0 \\ 0 & 0 & -6.2982 \times 10^{-5} & 0 \\ 0 & 0 & 0 & -0.43268 \end{bmatrix}, \tag{27}$$

and

$$H_1(Z;\, \epsilon) = \begin{bmatrix} H_{11} \\ H_{12} \\ H_{13} \\ H_{14} \end{bmatrix} = \begin{bmatrix} -361466.6608 z_1 \epsilon + 609227.5836 z_2 \epsilon + h_1(z_1,\, z_2,\, z_3,\, z_4,\, \epsilon) \\ -59002.8003 z_1 \epsilon + 99445.2251 z_2 \epsilon + h_2(z_1,\, z_2,\, z_3,\, z_4,\, \epsilon) \\ h_3(z_1,\, z_2,\, z_3,\, z_4,\, \epsilon) \\ h_4(z_1,\, z_2,\, z_3,\, z_4,\, \epsilon) \end{bmatrix}. \tag{28}$$

Functions $h_i(z_1,\, z_2,\, z_3,\, z_4)$ for $i = 1,\, 2,\, 3,\, 4$ are polynomials with the rest of higher order terms. The associated Hopf bifurcation normal form truncated at the third order term can be written as

$$\begin{aligned} \frac{dr}{dt'} &= r(v_0 \epsilon + v_1 r^2), \\ \frac{d\theta}{dt'} &= \omega_0 + \tau_0 \epsilon + \tau_1 r^2. \end{aligned} \tag{29}$$

Here, t' is a new time variable, $\omega_0 = 0.039358$, v_0 and τ_0 are determined as follows

$$v_0 = \frac{d\alpha(\epsilon)}{d\epsilon}|_{\epsilon=0} = \frac{1}{2}\left(\frac{\partial^2 H_{11}}{\partial z_1 \partial \epsilon} + \frac{\partial^2 H_{12}}{\partial z_2 \partial \epsilon}\right)_{z_i=0,\, \epsilon=0} = -131010.7179, \tag{30}$$

where$[\alpha(\epsilon) + i\omega(\epsilon)]|_{\epsilon=0} = i\omega_0$ is one of pure imaginary eigenvalue pair at Hopf critical point. Setting the system (26) with $\epsilon = 0$ as input functions to the normal form computation program from [Yu, 1998], we have

$$v_1 = 4.4335 \times 10^{-17}, \quad \tau_1 = -1.3073 \times 10^{-19}. \tag{31}$$

The equilibrium solutions of the first equation of (29) are $\bar{r}_0 = 0$ and $\bar{r}_1$. Here $\bar{r}_1$ is determined by

$$f_1(r;\, \epsilon) = v_0 \epsilon + v_1 r^2 = 0 \quad \Rightarrow \quad r^2 = -\frac{v_0\, \epsilon}{v_1}. \tag{32}$$

Since $v_0 < 0$ and $v_1 > 0$, the positiveness of r^2 asks $\epsilon > 0$. The stability is determined by the derivative of the right side of the first equation in (29). Since

$$d(r\, f_1(r;\, \epsilon)) = \frac{d}{dr}(v_0 \epsilon r + v_1 r^3) = 3 r^2 v_1 + \epsilon v_0 = -2\, \epsilon\, v_0 > 0, \quad \epsilon > 0. \tag{33}$$

unstable limit cycles bifurcate from the subcritical Hopf bifurcation on the $\epsilon > 0$ direction. With the presence of unstable DFE, stable endemic equilibrium, and unstable limit cycle, solutions either converge to stable equilibrium or a stable limit cycle. The persistence of the oscillation allows model (4) to exhibit multi-annual outbreak cycles. Numerical simulations are presented in Figure 3.

5.3. *Bogdanov-Takens bifurcation computation*

Taking parameter values from Table (1), model (4) exibits a Bogdanov-Takens bifurcation at the equilibrium $(S_{BT},\, I_{BT},\, R_{BT},\, B_{BT})$, where

$$S_{BT} = 1.216982139 \times 10^7,\, I_{BT} = 2451.903051,\, R_{BT} = 174966.6997,\, B_{BT} = 105081.5593, \tag{34}$$

when bifurcation parameters are

$$\beta_{E_{BT}} = 6.498914739 \times 10^{-11}, \quad \beta_{H_{BT}} = 1.617442248 \times 10^{-8}. \tag{35}$$

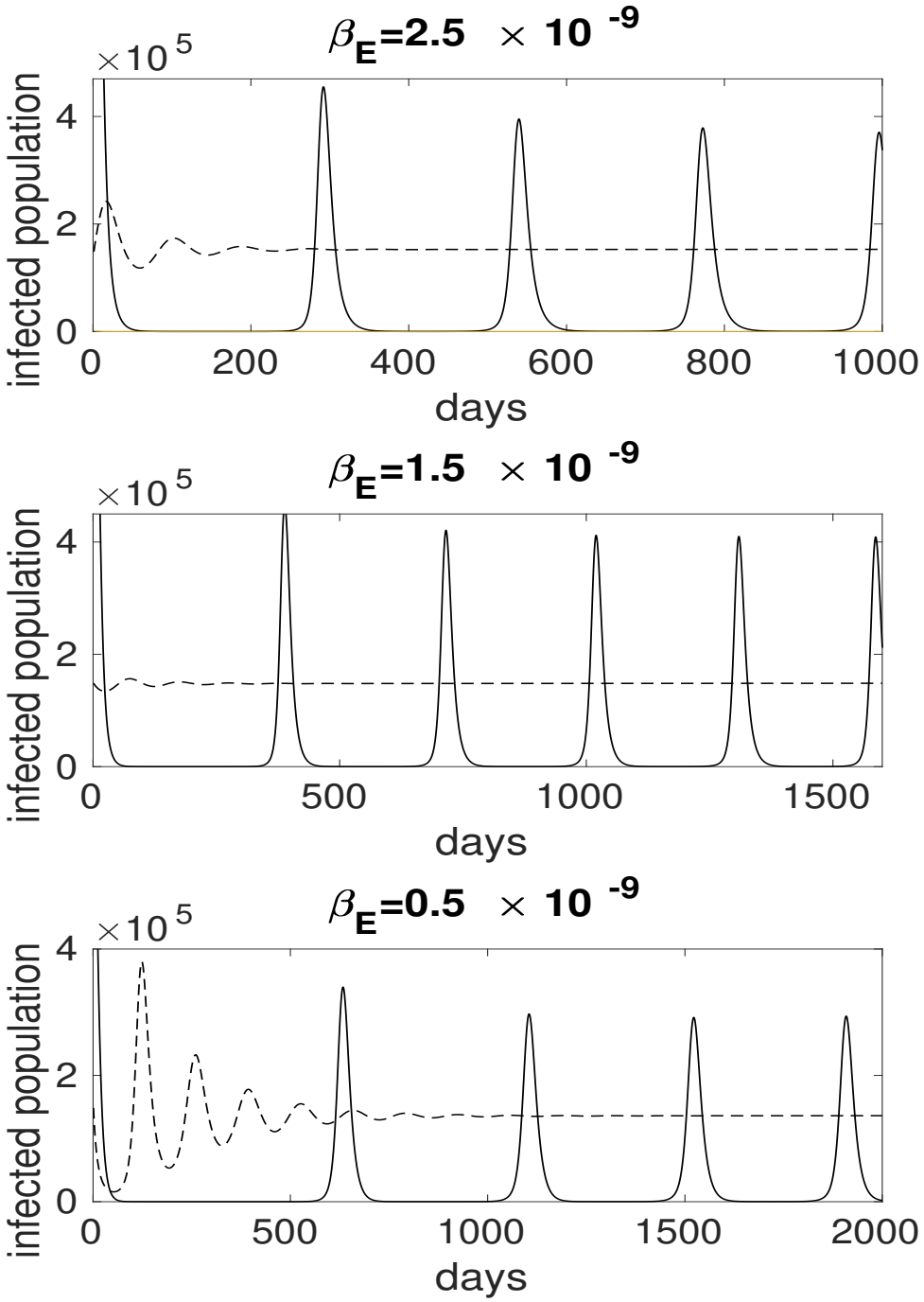

Fig. 3. Infected population size either stabilized on a relative high level (dashed line) with a high initial bacterium level 6×10^6, or outbreaks (solid curve) every one or two years with a low initial bacterium level 10. Simulation parameter values are taken from Table 1 and $\beta_H = 1.57 \times 10^{-7}$, $\beta_H = 1.2 \times 10^{-7}$, $\beta_H = 8 \times 10^{-8}$, respectively.

Take state variable transformation

$$\begin{bmatrix} S \\ I \\ R \\ B \end{bmatrix} = T \begin{bmatrix} y_1 \\ y_2 \\ y_3 \\ y_4 \end{bmatrix} + \begin{bmatrix} S_{BT} \\ I_{BT} \\ R_{BT} \\ B_{BT} \end{bmatrix},$$

where

$$T = \begin{bmatrix} -1.68316706827 & -1.693704558668 & -1.68839762629 & -1.31985415006453 \\ 0.023334226076 & 0.0233324305641 & 0.023333445456 & 0.0233961316797 \\ 1.6598328421939 & 1.67037212810428 & 1.6650641808346 & 1.296458018384829 \\ 1 & 1 & 1 & 1 \end{bmatrix}. \tag{36}$$

System (4) at $(\beta_{E_{BT}}, \beta_{H_{BT}})$ is transformed to

$$\dot{y} = G(y) = A\,y + \frac{1}{2}B(y,\, y) + O(\|y\|^3), \tag{37}$$

where $y = (y_1,\, y_2,\, y_3,\, y_4)^{tr}$,

$$A = \begin{bmatrix} -0.629822075264 & 0 & 0 & 0 \\ 0 & -0.2393996333732 & 0 & 0 \\ 0 & 0 & 0 & 6.4389141840704 \times 10^{-4} \\ 0 & 0 & 0 & 0 \end{bmatrix},$$

and the row elements of $B(y,\, y)$ are $B_i(x,\, y) = \sum_{j,k=1}^{n} \dfrac{\partial^2 G_i(\eta)}{\partial \eta_j \partial \eta_k}\Big|_{\eta=0} x_j y_k$. System (37) has equilibrium $y = 0$ with two eigenvalues $\lambda_{1,2} = 0$, which shows a Bogdanov-Takens bifurcation. For two zero eigenvalues, two real gneralized eigenvalues, satisfying $Aq_0 = 0$ and $Aq_1 = q_0$, are calculated as $q_0 = (0,\, 0,\, 1,\, 0)^T$ and $q_1 = (0,\, 0,\, 0,\, 1553.056884)^T$. Moreover, similar vectors for the transposed matrix A^T, satisfying $A^T p_1 = 0$ and $A^T p_0 = p_1$, are

$$p_0 = (0,\, 0,\, 1,\, 0)^{tr}, \quad p_1 = (0,\, 0,\, 0,\, 0.0006438914184)^{tr}. \tag{38}$$

The selected vectors satisfies $< p_0, q_0 >=< p_1, q_1 >= 1$ and $< p_0, q_1 >=< p_1, q_0 >= 0$, where $< \cdot, \cdot >$ is the inner product. Applying the formulas in [Kuznetsov, 2005], we have

$$B(q_0, q_0) = \begin{bmatrix} 0.000672187022394 \\ 0.000612772889621 \\ -0.001284244046664 \\ -7.1586363562 \times 10^{-7} \end{bmatrix},\ B(q_0, q_1) = \begin{bmatrix} 0.0024558963333 \\ 0.00223882249795 \\ -0.0046921009117 \\ -2.615420515341 \times 10^{-6} \end{bmatrix} \tag{39}$$

$$\tilde{a}_2 = \frac{1}{2} < p_1, B(q_0, q_0) >= -0.2304692258637 \times 10^{-9},$$

$$\tilde{b}_2 =< p_0, B(q_0, q_0) > + < p_1, B(q_0, q_1) >= -0.0012842457307.$$

Therefore, system (4) has a generic Bogdanov-Takens bifurcation at the equilibrium $(S_{BT},\, I_{BT},\, R_{BT},\, B_{BT})$ with bifurcation parameters taking $(\beta_{E_{BT}},\, \beta_{H_{BT}})$ and other parameters taking from Table 1. Its local unfolding is topologically equivalent to the canonical family

$$\dot{\zeta_1} = \zeta_2, \quad \dot{\zeta_2} = \tilde{\beta}_1 + \tilde{\beta}_2 \zeta_1 + \tilde{a}_2 \zeta_1^2 + \tilde{b}_2 \zeta_1 \zeta_2. \tag{40}$$

6. Infected peak in outbreaks

6.1. *The influence from transmission rates*

The reported infected cases in 2008–2009 Zimbabwe cholera epidemic is $98,585$, that is approximately 10^6 [Cuneo *et al.*, 2017]. Due to the asymptomatic infected cases, which are approximately half of the total infected cases[Nelson *et al.*, 2009], the total infected population peak can be approximately in the order of 10^6. We also investigate the control in the human-to-human transmission route by examining the relation between the transmission rate β_H and infected population peak. Numerical simulations on infected peak vs β_H are plotted in Figure 4. The simulation indicates that the peak of the outbreak increases as the infection rate β_H increases and then becomes saturated.

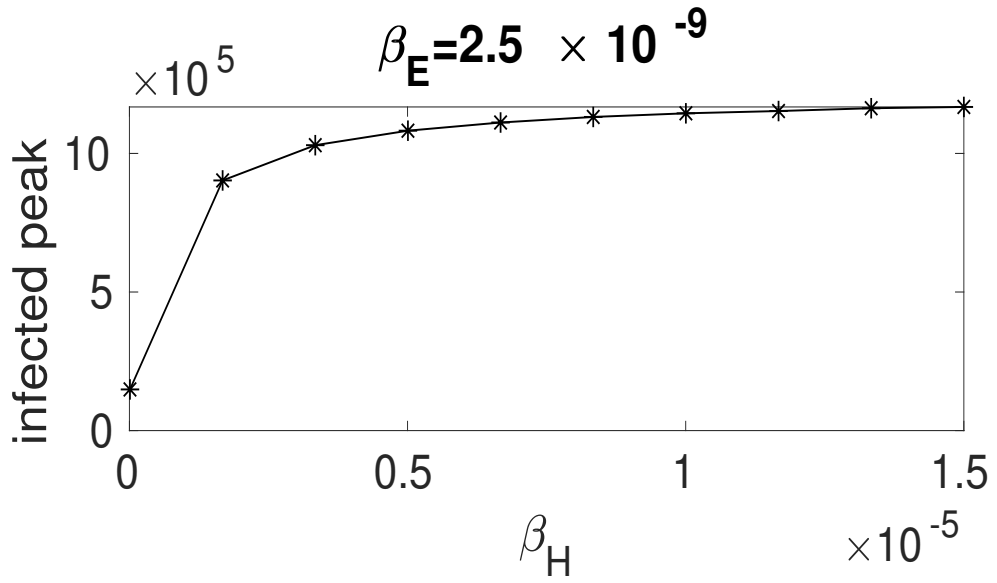

Fig. 4. Infected peak vs β_H

6.2. *Seasonal influence on the environment-human transmission pathway*

Transmission rate can be driven by many factors, such as the environmental variations for the growth of the bacterium [Pascual *et al.*, 2000, 2002] and human immune competence against the bacterium invasion [Greenwood, 1999; Sultan *et al.*, 2005]. Seasonal transmission rates therefore are assumed to be sinusoidal for the mathematical convenience [Grassly & Fraser, 2006] as

$$\beta_E(t) = \beta_E \left(1 + A_E \sin(\omega t)\right), \tag{41}$$

where $A_E \in [0, 1]$ denotes the strengths of seasonal forcing and measures the amplitude of the seasonality in environment-human transmission pathway. ω is approximately taken $(2\pi/365)$ as in [Posny & Wang, 2014]. Simulated infected population in Figure 5 shows that environmental seasonality affects the outbreak amplitudes.

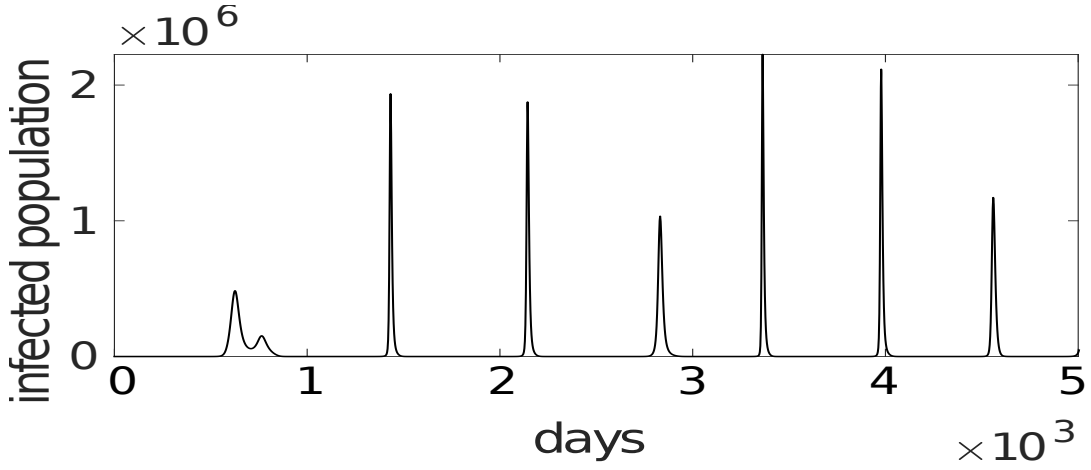

Fig. 5. Outbreaks influenced by seasonality in environmental-to-human transmission route. Here $\beta_H = 3 \times 10^{-8}$ and $\beta_E = (1 + \sin \frac{2\pi t}{365}) \times 2.5 \times 10^{-9}$.

7. Concluding Remarks

In this work, we formulate a simple ODE model for cholera transmission to recover periodic re-emerging outbreak patterns in cholera endemic region. The model is an extension of the classical SIRS model including a bacterial compartment B. The model incorporates direct human-to-human transmission in the simple mass-action form and indirect environmental-to-human transmission considering the non-homogeneous interaction. Specifically, the host-pathogen encounter is modeled by a pure birth process to account for the randomness in the encounter-searching distance. This novel encounter rate results in a non-linear incidence rate, which is a special case of a general nonlinear incidence form proposed by [Hethcote & Van den Driessche, 1991]. Consequently, the developed model (4) not only exhibits disease-free and persist stages of the infection, but also shows oscillating re-emerging outbreaks with long quiescent periods. Therefore, this modeling framework provides a new approach to study periodic outbreaks for cholera and emergence and re-emergence for other infectious diseases with multiple transmission routes.

Model (4) is thoroughly analyzed. Our results show that there exist two threshold values, $\beta_H = \beta_{Ht}$ and $\beta_E = \beta_{Et}$, for direct and indirect transmissions to determine the number of equilibrium solutions and critical conditions for transcritical and backward bifurcations. Particularly, model (4) allows at most three biologically feasible equilibria. $\beta_H = \beta_{Ht}$ is the critical value for a transcritical bifurcation, at which the model further induces a backward bifurcation when $\beta_E > \beta_{Et}$ and a forward bifurcation when $\beta_E < \beta_{Et}$. Moreover, the global stability of the DFE and endemic equilibirum are established by using Lyapunov function method and geometric metric approach, respectively. Since the occurrence of backward bifurcation indicates the existence of bi-stability, model (4) may exhibit the bi-stable behavior in epidemiology. Our analytical results indicate that environmental reservoir of *Vibrio cholerae* is a cause of the disease outbreak. Additionally, the existence of environmental-living pathogens rises up the difficulty of disease elimination, since the disease-completely-eliminating threshold R_2 in (16) is a positive function of the bacteria shedding rate ξ. The global stability of disease-free state is more difficult to reach. Besides, the global stability of endemic equilibrium also rarely happens, which in turn leads to complex dynamical behaviors of our model, such as oscillations and multiple stability. The global stability analyses are presented in Theorems 3 and 4.

Complex dynamics are further demonstrated in 2-dimensional bifurcation diagrams. Saddle-node, transcritical, and Hopf bifurcation curves delimit 2-dimensional parameter planes into three parts. In these three parameter regions, model (4) admits one, three, and two equilibrium solutions, which correspond to globally stable DFE, bi-stable state, and coexisting state of an endemic equilibrium and unstable DFE, respectively. Moreover, our simple model (4) exhibits backward, Hopf, and Bogdanov-Takens bifurcations, which is due to the novel formulation of transmission probability between the bacteria and human hosts. The Hopf bifurcation, particularly, provides an oscillatory source and captures multi-annual disease outbreaks. However, the period and amplitude of the periodic outbreaks are uni-variant, as these behaviors are generated intrinsically from an autonomous model. Varying outbreak periods and amplitudes can be achieved by further considering exogenous forces, such as seasonality. Our results highlight we underscore the gap between the complex mechanism of cholera transmission and our current quantitative understanding and control strategies for this disease.

Although we have considered demographic and environmental variability, there are other factors of variability that could be incorporated in a more comprehensive model. An important example among these is the individual heterogeneity in shedding density and the possibility of super-shedding and hyper-infectivity of the bacteria. The impact of such individual heterogeneity in shedding and infectivity on cholera epidemics will provide an interesting topic in future research.

Acknowledgement

The author would like to acknowledge Dr. Xueying Wang from Washington State University for a complete revision of the entire manuscript including clarification of explanations, verification of results, and corrections of spelling and grammar errors. The author also thanks Dr. Xueying Wang, Dr. Leif Ellingson from Texas Tech University, and Dr. Lindi Wahl from Western University for discussions and suggestions for the formulation of probability of indirect transmission.

References

Andrews, J. R. & Basu, S. [2011] "Transmission dynamics and control of cholera in haiti: an epidemic model," *The Lancet* **377**, 1248–1255.

Arino, J., McCluskey, C. C. & van den Driessche, P. [2003] "Global results for an epidemic model with vaccination that exhibits backward bifurcation," *SIAM Journal on Applied Mathematics* **64**, 260–276.

Ballyk, M. M., McCluskey, C. C. & Wolkowicz, G. S. [2005] "Global analysis of competition for perfectly substitutable resources with linear response," *Journal of Mathematical Biology* **51**, 458–490.

Capasso, V. & Paveri-Fontana, S. [1979] "A mathematical model for the 1973 cholera epidemic in the european mediterranean region." *Revue d'épidémiologie et de Santé Publiqué* **27**, 121–132.

Castillo-Chavez, C. & Song, B. [2004] "Dynamical models of tuberculosis and their applications." *Mathematical Biosciences and Engineering: MBE* **1**, 361.

Codeço, C. T. [2001] "Endemic and epidemic dynamics of cholera: the role of the aquatic reservoir," *BMC Infectious Diseases* **1**, 1.

Costello, W. G. & Taylor, H. M. [1975] "Mathematical models of the sterile male technique of insect control," *Mathematical Analysis of Decision Problems in Ecology* (Springer), pp. 318–359.

Cuneo, C. N., Sollom, R. & Beyrer, C. [2017] "The cholera epidemic in zimbabwe, 2008–2009: a review and critique of the evidence," *Health and Human Rights* **19**, 249.

Dennis, B. [1989] "Allee effects: population growth, critical density, and the chance of extinction," *Natural Resource Modeling* **3**, 481–538.

DiRita, V. J. [1995] "Vibrio cholerae and cholera: molecular to global perspectives: edited by I. Kaye Wachsmuth, Paul A. Blake and ørjan Olsvik ASM Press, 1994. (xii+ 465 pages) ISBN 1 55581 067 5," *Trends in Microbiology* **3**, 79–80.

Feng, X., Ruan, S., Teng, Z. & Wang, K. [2015] "Stability and backward bifurcation in a malaria transmission model with applications to the control of malaria in China," *Mathematical Biosciences* **266**, 52–64.

Freedman, H. I., Ruan, S. & Tang, M. [1994] "Uniform persistence and flows near a closed positively invariant set," *Journal of Dynamics and Differential Equations* **6**, 583–600.

Ghosh, M., Chandra, P., Sinha, P. & Shukla, J. [2004] "Modelling the spread of carrier-dependent infectious diseases with environmental effect," *Applied Mathematics and Computation* **152**, 385–402.

Glass, R. I., Becker, S., Huq, M. I., Stoll, B. J., Khan, M., Merson, M. H., Lee, J. V. & Black, R. E. [1982] "Endemic cholera in rural bangladesh, 1966–1980," *American Journal of Epidemiology* **116**, 959–970.

Grassly, N. C. & Fraser, C. [2006] "Seasonal infectious disease epidemiology," *Proceedings of the Royal Society of London B: Biological Sciences* **273**, 2541–2550.

Greenwood, B. [1999] "Meningococcal meningitis in Africa," *Transactions of the Royal Society of Tropical Medicine and Hygiene* **93**, 341–353.

Hartley, D. M., Morris Jr, J. G. & Smith, D. L. [2005] "Hyperinfectivity: a critical element in the ability of V. cholerae to cause epidemics?" *PLoS Medicine* **3**, e7.

Hethcote, H. W. & Van den Driessche, P. [1991] "Some epidemiological models with nonlinear incidence," *Journal of Mathematical Biology* **29**, 271–287.

Islam, S., Rheman, S., Sharker, A., Hossain, S., Nair, G., Luby, S., Larson, C. & Sack, D. [2009] "Climate change and its impact on transmission dynamics of cholera," *Climate Change Cell, DoE, MoEF* .

King, A. A., Ionides, E. L., Pascual, M. & Bouma, M. J. [2008] "Inapparent Infections and Cholera Dynamics," *Nature* **454**, 877.

Kuznetsov, Y. A. [2005] "Practical computation of normal forms on center manifolds at degenerate bogdanov–takens bifurcations," *International Journal of Bifurcation and Chaos* **15**, 3535–3546.

Li, M. Y. [2018] *An Introduction to Mathematical Modeling of Infectious Diseases*, Vol. 2 (Springer).

Li, M. Y. & Muldowney, J. S. [1995] "On RA Smith's autonomous convergence theorem," *The Rocky Mountain Journal of Mathematics* , 365–379.

Li, M. Y. & Muldowney, J. S. [1996] "A geometric approach to global-stability problems," *SIAM Journal on Mathematical Analysis* **27**, 1070–1083.

Lu, G. & Lu, Z. [2012] "Geometric approach for global asymptotic stability of three-dimensional Lotka–

Volterra systems," *Journal of Mathematical Analysis and Applications* **389**, 591–596.

Lu, G. & Lu, Z. [2017] "Geometric approach to global asymptotic stability for the SEIRS models in epidemiology," *Nonlinear Analysis: Real World Applications* **36**, 20–43.

Martin Jr, R. H. [1974] "Logarithmic norms and projections applied to linear differential systems," *Journal of Mathematical Analysis and Applications* **45**, 432–454.

Merrell, D. S., Butler, S. M., Qadri, F., Dolganov, N. A., Alam, A., Cohen, M. B., Calderwood, S. B., Schoolnik, G. K. & Camilli, A. [2002] "Host-induced epidemic spread of the cholera bacterium," *Nature* **417**, 642.

Morris Jr, J. G. [2011] "Cholera—modern pandemic disease of ancient lineage," *Emerging Infectious Diseases* **17**, 2099.

Mukandavire, Z., Liao, S., Wang, J., Gaff, H., Smith, D. L. & Morris, J. G. [2011] "Estimating the reproductive numbers for the 2008–2009 cholera outbreaks in Zimbabwe," *Proceedings of the National Academy of Sciences* **108**, 8767–8772.

Muldowney, J. S. [1984] "Dichotomies and asymptotic behaviour for linear differential systems," *Transactions of the American Mathematical Society* **283**, 465–484.

Muldowney, J. S. [1990] "Compound matrices and ordinary differential equations," *The Rocky Mountain Journal of Mathematics* , 857–872.

Neilan, R. L. M., Schaefer, E., Gaff, H., Fister, K. R. & Lenhart, S. [2010] "Modeling optimal intervention strategies for cholera," *Bulletin of Mathematical Biology* **72**, 2004–2018.

Nelson, E. J., Harris, J. B., Morris Jr, J. G., Calderwood, S. B. & Camilli, A. [2009] "Cholera transmission: the host, pathogen and bacteriophage dynamic," *Nature Reviews Microbiology* **7**, 693.

Organization, W. H. [2010] ""cholera vaccines: Who position paper," *Wkly Epidemiol Rec* **85**, 117–128.

Pascual, M., Bouma, M. J. & Dobson, A. P. [2002] "Cholera and climate: revisiting the quantitative evidence," *Microbes and Infection* **4**, 237–245.

Pascual, M., Rodó, X., Ellner, S. P., Colwell, R. & Bouma, M. J. [2000] "Cholera dynamics and El Nino-southern oscillation," *Science* **289**, 1766–1769.

Ponciano, J. M. & Capistrán, M. A. [2011] "First principles modeling of nonlinear incidence rates in seasonal epidemics," *PLoS Computational Biology* **7**, e1001079.

Posny, D. & Wang, J. [2014] "Modelling cholera in periodic environments," *Journal of Biological dynamics* **8**, 1–19.

Robertson, S. L., Eisenberg, M. C. & Tien, J. H. [2013] "Heterogeneity in multiple transmission pathways: modelling the spread of cholera and other waterborne disease in networks with a common water source," *Journal of Biological Dynamics* **7**, 254–275.

Sack, D. A., Sack, R. B., Nair, G. B. & Siddique, A. [2004] "Cholera," *The Lancet* **363**, 223–233.

Silva, A. J. & Benitez, J. A. [2016] "Vibrio cholerae biofilms and cholera pathogenesis," *PLoS Neglected Rropical Diseases* **10**, e0004330.

Smith, H. L., Wang, L. & Li, M. Y. [2001] "Global dynamics of an SEIR epidemic model with vertical transmission," *SIAM Journal on Applied Mathematics* **62**, 58–69.

Sultan, B., Labadi, K., Guégan, J.-F. & Janicot, S. [2005] "Climate drives the meningitis epidemics onset in West Africa," *PLoS Medicine* **2**, e6.

Tian, J. P., Liao, S. & Wang, J. [2013] "Analyzing the infection dynamics and control strategies of cholera," (Conference Publications).

Tien, J. H. & Earn, D. J. [2010] "Multiple transmission pathways and disease dynamics in a waterborne pathogen model," *Bulletin of Mathematical Biology* **72**, 1506–1533.

Tien, J. H., Poinar, H. N., Fisman, D. N. & Earn, D. J. [2010] "Herald waves of cholera in nineteenth century london," *Journal of The Royal Society Interface* , rsif20100494.

van den Driessche, P. & Watmough, J. [2002] "Reproduction numbers and sub-threshold endemic equilibria for compartmental models of disease transmission," *Mathematical Biosciences* **180**, 29–48.

Wandiga, S., Opondo, M., Kathuri, J., Olago, D., Apindi, E., Olaka, L., Githeko, A., Githui, F., Opere, A., Ogallo, L. *et al.* [2006] "Climate change induced vulnerability to malaria and cholera in the lake victoria region," *A final report submitted to assessments of impacts and adaptations to climate change (AIACC), project no. AF91. Washington, DC: The International START Secretariat* .

Wang, X. & Wang, J. [2015] "Analysis of cholera epidemics with bacterial growth and spatial movement," *Journal of Biological Dynamics* **9**, 233–261.

Yu, P. [1998] "Computation of normal forms via a perturbation technique," *Journal of Sound and Vibration* **211**, 19–38.

Yu, P. [2005] "Closed-form conditions of bifurcation points for general differential equations," *International Journal of Bifurcation and Chaos* **15**, 1467–1483.

Appendix A

A derivation of (1): By (H1), the probability density function of discrete random variable $X(a)$ is

$$p_i(a) = \mathbb{P}\{X(a) = i\} = \mathbb{P}\{X(a) = i | X(0) = 0\}$$

and the transition probability

$$p_{ij}(a) = \mathbb{P}\{X(a) = i | X(0) = j\}.$$

Hence $p_{i0} = p_i(a)$. It follows from (H1)-(H3) that

$$\begin{aligned} p_{00}(a + \Delta a) &= p_0(a + \Delta a) \\ &= \mathbb{P}\{X(a) = 0,\, X(a + \Delta a) - X(a) = 0\} \\ &= \mathbb{P}\{X(a) = 0\}\, \mathbb{P}\{X(a + \Delta a) - X(a) = 0\} \\ &= \mathbb{P}\{X(a) = 0\}\, \mathbb{P}\{X(\Delta a) - X(0) = 0\} \\ &= \mathbb{P}\{X(a) = 0\}\, \mathbb{P}\{X(\Delta a) = 0\}, \end{aligned}$$

Hence,

$$p_0(a + \Delta a) = p_{00}(a + \Delta a) = p_0(a)\, p_0(\Delta a) = p_0(a)\, \left[1 - h\,(B)\, \Delta a + o(\Delta a)\right].$$

For the previous equation, subtracting $p_0(a)$ from both sides and dividing by Δa yields

$$\frac{p_0(a + \Delta a) - p_0(a)}{\Delta a} = -h(B) p_0(a) + \frac{o(\Delta a)}{\Delta a} p_0(a).$$

Taking the limit as $\Delta a \to 0$ leads to the following first-order differential equation

$$\frac{dp_0(a)}{da} = -h(B) p_0(a),$$

with initial condition $p_0(0) = \mathbb{P}\{X(0)\} = 1$. The solution of the preceding linear differential equation is

$$p_0(a) = e^{-ah(B)}.$$

Appendix B

Estimate parameter ranges for β_H and β_E: Public awareness and improved sanitation efforts are prompted control strategies to prevent cholera spreading. Therefore, β_H is set as a free parameter (or bifurcation parameter) and examined for its influence on the cholera dynamics. As to $\hat{\beta}_E$, the value of $\beta_E = c_0\, \hat{\beta}_E$ is estimated by the indirect transmission rate β_e [Mukandavire *et al.*, 2011] from the 2008-2009 cholera outbreak in Zimbabwe. Since the model [Mukandavire *et al.*, 2011] takes the density-dependent contact rate, we have $\beta_e/(\bar{B} + K) = \mathcal{O}\left(\beta_E\, \bar{B}/(\bar{B} + K)\right)$ and $\beta_e \in (0.075, 2.1)$. The infected population size is stabilized at $\bar{I} = 1 \times 10^5$ cases. Then the estimated stablized bacterial concentration is $\bar{B} = \frac{\xi}{\delta} \bar{I} = 3 \times 10^7$ cell $\cdot$ L^{-1}. The estimated range for β_E is $(0.25 \times 10^{-8},\, 7 \times 10^{-8})$.

Appendix C: The Geometric Approach

We summarize the main result of the geometric approach based on the second additive compound matrix, originally developed by Li and and Muldowney [Li & Muldowney, 1996].

For a 4×4 matrix $M = (m_{ij})$, its second additive compound matrix is

$$M^{[2]} = \begin{bmatrix} m_{11}+m_{22} & m_{23} & m_{24} & -m_{13} & -m_{14} & 0 \\ m_{32} & m_{11}+m_{33} & m_{34} & m_{12} & 0 & -m_{14} \\ m_{42} & m_{43} & m_{11}+m_{44} & 0 & m_{12} & m_{13} \\ -m_{31} & m_{21} & 0 & m_{22}+m_{33} & m_{34} & -m_{24} \\ -m_{41} & 0 & m_{21} & m_{43} & m_{22}+m_{44} & m_{23} \\ 0 & -m_{41} & m_{31} & -m_{42} & m_{32} & m_{33}+m_{44} \end{bmatrix}$$

The readers can refer to a survey of general compound matrices [Muldowney, 1990].

Consider a dynamical system

$$\frac{dX}{dt} = f(X) \tag{42}$$

where $f : D \mapsto \mathbb{R}^n$ is a C^1 function and $D \subset \mathbb{R}^n$ is a simply connected open set. Let $X \mapsto A(X)$ be a $\binom{n}{2} \times \binom{n}{2}$ matrix-valued C^1 function in D, and set

$$B = A_f A^{-1} + A J^{[2]} A^{-1} ,$$

where A_f is the derivative of A (entry-wise) along the direction of f, and $J^{[2]}$ is the second additive compound matrix of the Jacobian $J(X) = Df(X)$. Let $M(B)$ be the Lozinskiĭ measure of B with respect to a matrix norm; that is,

$$M(B) = \lim_{h \to 0^+} \frac{|\mathbb{I} + hB| - 1}{h} ,$$

where $\mathbb{I}$ is the identity matrix. Define a quantity $\bar{q}_2$ as

$$\bar{q} = \limsup_{t \to \infty} \sup_{X_0 \in K} \frac{1}{t} \int_0^t M\big(B(X(s, X_0))\big)\, ds , \tag{43}$$

where K is a compact absorbing subset of D. Then the condition $\bar{q} < 0$ provides a Bendixson criterion in D. Consequently, the following theorem holds:

Theorem 5.

Suppose that there exists a compact absorbing set $K \subset D$ and the system (42) has a unique equilibrium point X^* in D. Then X^* is globally asymptotically stable in D if $\bar{q} < 0$.